



Impact of Window Opening Shapes on Wind-Driven Cross Ventilation Performance in a Generic Isolated Building: A Simulation Study

Burak AKTEPE¹ , Hacımurat DEMİR^{1*} 

¹Aksaray University, Engineering Faculty, Department of Mechanical Engineering, Aksaray, Turkey

Article Info

Research article
Received: 30/07/2024
Revision: 28/08/2024
Accepted: 28/08/2024

Keywords

CFD
Natural Ventilation
Building Aerodynamics
Ventilation Rate
Atmospheric Boundary
Layer

Makale Bilgisi

Araştırma makalesi
Başvuru: 30/07/2024
Düzeltilme: 28/08/2024
Kabul: 28/08/2024

Anahtar Kelimeler

CFD
Doğal Havalandırma
Bina Aerodinamiği
Havalandırma Oranı
Atmosferik Sınır Tabaka

Graphical/Tabular Abstract (Grafik Özet)

In this study, the effects of wind-induced cross ventilation in a generic isolated building with various window opening geometries including rectangular, trapezoidal, triangular and hexagonal were numerically examined. / Bu çalışmada, dikdörtgen, trapez, üçgen ve altıgen olmak üzere çeşitli pencere açıklık geometrilerine sahip genel bir izole binada rüzgar kaynaklı çapraz havalandırmanın etkileri sayısal olarak incelenmiştir.

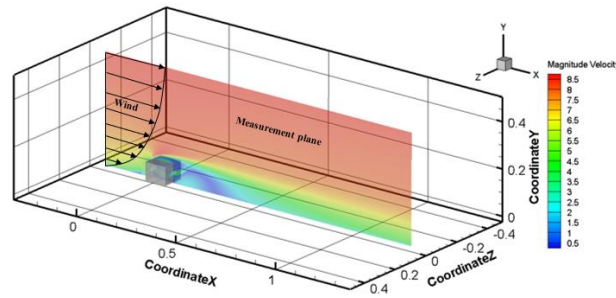


Figure A: Contour measurement plane at the building center / Şekil A: Bina merkezindeki kontur ölçüm düzlemi

Highlights (Önemli noktalar)

- Jet spreading size varied with geometry. / Jet yayılma boyutu geometriye göre değişmiştir.
- Reference geometry achieved the highest ventilation rate (0.004212 m³/s), followed by trapezoidal, hexagonal, and triangular. / Referans geometri en yüksek havalandırma oranına (0,004212 m³/s) ulaşmış, bunu trapez, altıgen ve üçgen takip etmiştir.
- Triangular geometry should be avoided for ventilation performance prioritization. / Havalandırma performansı önceliklendirmesi için üçgen geometriden kaçınılmalıdır.

Aim (Amaç): The aim of this study is to present a numerical investigation of natural wind-driven cross ventilation in an isolated building with a variety of window opening shapes. / Bu çalışmanın amacı, çeşitli pencere açıklık şekillerine sahip izole bir binada doğal rüzgar tahrikli çapraz havalandırmanın sayısal bir incelemesini sunmaktır.

Originality (Özgünlük): The originality of this study is that natural wind-induced cross ventilation is numerically investigated in an isolated building with various window opening shapes, beyond the existing literature which usually focuses only on rectangular geometries. / Bu çalışmanın özgünlüğü, mevcut literatürde genellikle yalnızca dikdörtgen geometrilere odaklanılmasının ötesinde, çeşitli pencere açıklık şekillerine sahip izole bir binada doğal rüzgar kaynaklı çapraz havalandırmanın sayısal olarak incelenmiş olmasıdır.

Results (Bulgular): The airflow velocity profile showed a U-shaped curve, with a reduction observed in all cases within the range of $0 < x/D < 0.5$. Trapezoid and reference geometries demonstrated similar decreases, while the hexagon curve remained relatively higher. All curves increased in the range $0.5 < x/D < 1$, reaching values of 0.6-0.7 near $x/D=1$. / Hava akış hızı profili U şeklinde bir eğri göstermiş ve $0 < x/D < 0,5$ aralığındaki tüm durumlarda bir azalma gözlemlenmiştir. Yamuk ve referans geometriler benzer düşüşler gösterirken, altıgen eğri nispeten daha yüksek kalmıştır. Tüm eğriler $0,5 < x/D < 1$ aralığında artarak $x/D=1$ yakınında 0,6-0,7 değerlerine ulaşmıştır.

Conclusion (Sonuç): In terms of ventilation rate, reference geometry exhibited the greatest performance (0.004212 m³/s), followed by trapezoidal, hexagonal, and triangular. It is recommended that triangular geometry be avoided in instances where ventilation performance is the primary objective. / Havalandırma oranı açısından, referans geometri en yüksek performansı (0,004212 m³/s) sergilemiş, bunu trapezoidal, altıgen ve üçgen takip etmiştir. Havalandırma performansının birincil hedef olduğu durumlarda üçgen geometriden kaçınılması tavsiye edilmektedir.



Impact of Window Opening Shapes on Wind-Driven Cross Ventilation Performance in a Generic Isolated Building: A Simulation Study

Burak AKTEPE¹ , Hacımurat DEMİR^{1*} ¹Aksaray University, Engineering Faculty, Department of Mechanical Engineering, Aksaray, Turkey

Article Info

Research article
Received: 30/07/2024
Revision: 28/08/2024
Accepted: 28/08/2024

Keywords

CFD
Natural Ventilation
Building Aerodynamics
Ventilation Rate
Atmospheric Boundary
Layer

Abstract

Both environmental concerns and sustainable development goals have led to the search for alternative energy-efficient solutions. Natural ventilation, a crucial aspect of energy-efficient building design, reduces dependence on mechanical systems and regulates indoor air quality and temperature using natural forces. It improves indoor air quality, reduces energy consumption, and lowers operating costs. This paper presents a computational fluid dynamics analysis of natural cross-ventilation in an isolated building with varying window opening geometries. u/u_{ref} showed a marked decrease in triangular geometries, while trapezoidal and reference geometries exhibited comparable declines. The airflow velocity profile revealed a U-shaped curve, with reductions observed within $0 < x/D < 0.5$ and increased in the range $0.5 < x/D < 1$. High-velocity jets entering from the windward side varied in height by geometry and triangular geometry produced the narrowest jet, while hexagonal geometry demonstrated the widest. Ventilation rate comparisons for different geometries showed the reference geometry as the most efficient ($0.004212 \text{ m}^3/\text{s}$), followed by trapezoidal ($0.003136 \text{ m}^3/\text{s}$), hexagonal ($0.003134 \text{ m}^3/\text{s}$), and triangular ($0.002158 \text{ m}^3/\text{s}$). These findings highlighted the significant impact of window geometry on building ventilation performance and underscored the importance of careful window design to optimize efficiency.

Genel İzole Bir Binada Pencere Açıklık Şekillerinin Rüzgar Kaynaklı Çapraz Havalandırma Performansına Etkisi: Bir Simülasyon Çalışması

Makale Bilgisi

Araştırma makalesi
Başvuru: 30/07/2024
Düzelme: 28/08/2024
Kabul: 28/08/2024

Anahtar Kelimeler

CFD
Doğal Havalandırma
Bina Aerodinamiği
Havalandırma Oranı
Atmosferik Sınır Tabaka

Öz

Hem çevresel kaygılar hem de sürdürülebilir kalkınma hedefleri, alternatif enerji verimli çözümlerin aranmasına yol açmıştır. Enerji tasarruflu bina tasarımının önemli bir yönü olan doğal havalandırma, mekanik sistemlere bağımlılığı azaltır ve doğal güçleri kullanarak iç mekân hava kalitesini ve sıcaklığını düzenler. İç mekân hava kalitesini iyileştirir, enerji tüketimini azaltır ve işletme maliyetlerini düşürür. Bu makale, farklı pencere açıklık geometrilerine sahip izole bir binada doğal çapraz havalandırmanın hesaplamalı akışkanlar dinamiği analizini sunmaktadır. u/u_{ref} üçgen geometrilerde belirgin bir düşüş gösterirken, trapez ve referans geometriler benzer düşüşler sergilemiştir. Hava akış hızı profili U şeklinde bir eğri ortaya koymuş, $0 < x/D < 0,5$ aralığında azalmalar gözlenmiş ve $0,5 < x/D < 1$ aralığında artmıştır. Rüzgar tarafından giren yüksek hızlı jetlerin yüksekliği geometriye göre değişmiş ve üçgen geometri en dar jeti üretirken, altıgen geometri en geniş jeti göstermiştir. Farklı geometriler için havalandırma oranı karşılaştırmaları referans geometrinin en verimli olduğunu ($0,004212 \text{ m}^3/\text{s}$), bunu trapez ($0,003136 \text{ m}^3/\text{s}$), altıgen ($0,003134 \text{ m}^3/\text{s}$) ve üçgen ($0,002158 \text{ m}^3/\text{s}$) takip ettiğini göstermiştir. Bu bulgular, pencere geometrisinin bina havalandırma performansı üzerindeki önemli etkisini vurgulamış ve verimliliği optimize etmek için dikkatli pencere tasarımının önemini altını çizmiştir.

1. INTRODUCTION (GİRİŞ)

Recently, increasing environmental concerns and sustainable development goals have necessitated a search for alternative, environmentally friendly solutions besides the intensive use of fossil fuels in energy production. The heating, ventilation, and air

conditioning (HVAC) system is responsible for a significant portion of energy consumption in buildings, accounting for approximately 60-70% of the total energy use in non-industrial buildings, including commercial and residential buildings. The heating and cooling demands of these buildings are major contributors to this energy consumption.

Furthermore, ventilation and infiltration account for a substantial portion of the overall energy consumption, ranging from 30% to 50%. In light of these observations, natural ventilation has emerged as a crucial aspect of energy-efficient building design [1]. This method reduces dependence on mechanical systems and regulates indoor air quality and temperature using natural forces. Natural ventilation is critical in terms of sustainability because it reduces energy consumption and carbon emissions.

Natural ventilation provides effective air circulation in buildings by utilizing natural phenomena such as wind, buoyancy, pressure differentials, and convection. Natural ventilation is generally classified into three main categories: cross ventilation, stack ventilation and hybrid systems. Cross ventilation is based on placing openings on opposite sides of a building or room to facilitate airflow driven by wind pressure differences. In stack ventilation, the buoyancy effect is employed, in which warm air rises and exits through higher openings while drawing in cooler air through lower openings. Furthermore, hybrid ventilation systems provide flexibility and improved efficiency by combining natural and mechanical ventilation for optimizing indoor climate control.

The importance of natural ventilation extends beyond its role in reducing energy consumption. Natural ventilation enables a notable reduction in the use of mechanical ventilation systems, which lowers energy consumption and operating costs. It also plays an important role in improving indoor air quality, which is vital for the health and well-being of building occupants. Cross-ventilation helps to improve air circulation, remove indoor pollutants, control humidity levels, and maintain a comfortable and healthy indoor environment. In order to obtain more detailed information about natural ventilation and cross ventilation in particular, in addition to experimental studies [2-12], the number of studies using computational fluid dynamics (CFD) methodology has been increasing recently [13-34]. CFD offers many distinct benefits when compared to other methods. Unlike many experimental approaches, such as Particle Image Velocimetry (PIV), CFD offers comprehensive data on the whole flow field. This means that it gives information on the important parameters at every location inside the computational domain. CFD circumvents the occasional conflict between similarity criteria in testing at reduced scales by enabling fully-sized simulations to be conducted. Additionally, CFD provides complete control over the boundary

parameters and facilitates the fast execution of parametric investigations [30].

Meroney [15] and Shirzadi et al. [17] both examined the accuracy and reliability of different turbulence models in CFD simulations for cross ventilation. Meroney [15] simulated both 2D and 3D simulations of the ambient and internal air flow pattern of building model in wind tunnel experiment performed by Karava [9] with various turbulence models (SST $k-\omega$, standard, and RNG $k-\epsilon$) using CFD and compared these simulations with the measurements in the wind tunnel experiments. The internal airflow characteristics showed minimal sensitivity to the choice of turbulence model, indicating that simpler models can be used with near accuracy. According to Perén et al. [31], the SST $k-\omega$ turbulence model was determined to be the most precise, with RNG $k-\epsilon$ turbulence model being second most accurate. They found that the angle at which the jet entered through the windows varied as the roof inclination angle increased, which was caused by the varying pressure distribution on the windward side of the building.

Shirzadi et al. [17] constructed a CFD model and validated based on the experimental data provided by Tominaga and Blocken [11], then the closing coefficients of the $k-\epsilon$ turbulence model were obtained through the application of stochastic optimization and Monte Carlo sampling methods. Additionally, the modified coefficients obtained by the systematic approach successfully simulated cross ventilation phenomena in buildings, reducing the airflow rate prediction errors to less than 8% compared to experiments.

Moey et al. [16] and Al-Aghbari et al. [24] investigated the influence of building openings and roof configurations on ventilation performance. Moey et al. [16] found that smaller input openings and larger outlet openings result in higher velocities at the inlet, leading to reduced pressure inside the building and improved ventilation. Consequently, it was determined that the aperture ratio had a significant impact on the interior air circulation. By utilizing the sRANS equations and $k-\omega$ SST turbulence model, Al-Aghbari et al. [24] discovered that raising the angle of the roof pitch leads to a rise in the velocity of indoor airflow. The greatest pressure coefficient was observed at the mid-upper opening position when the roof pitch was set at a low angle of 9° . The mid-upper span configuration with a roof pitch angle of 27° exhibited the highest volumetric flow rate. In contrast, the lower-upper span location had a lower coefficient of pressure comparing the lower-middle span location due to

the presence of additional flow resistance caused by the different span locations.

Shirzadi et al. [18] and Tong et al. [19] focused on complex urban configurations and their influence on ventilation. Shirzadi et al. [18] investigated cross ventilation in high-density urban configurations using CFD models validated by the LES technique. The study compared the average flow characteristics, turbulence statistics, wind pressure and cross-air flow velocity for nine identical building models (3x3) and one surrounded building model for different planar area ratios ($0 \leq \lambda_p \leq 0.6$) and wind angles. For medium and high-density building configurations, the LES model was found to be more accurate than sRANS in predicting mean velocity and turbulent kinetic energy in the vicinity of and within building. It is also observed that for high-density urban configurations, the instantaneous ventilation velocity is significantly higher than the average velocity of airflow over time and is not affected by the direction of the wind. Besides, Tong et al. [19] used combined indoor-outdoor CFD simulations to look at how different urban parameters, like wind speed, building aspect ratios, and the presence of downstream obstacles, affect air exchange rates in different types of urban spaces. They concluded that fewer perimeter layers are needed for buildings that are taller than their surroundings, especially at high floors, that downstream buildings have less impact on ACH than upstream buildings, and that modeling only the adjacent building layer is insufficient due to the artificial duct effect between buildings.

Zobaied et al. [20] and Moey et al. [21] extended the investigation to specific building design features, including roof pitch and configuration. Zobaied et al. [20] conducted a numerical analysis using the sRANS equations and the SST k- ω turbulence model to investigate the airflow characteristics around building with different roof pitches of 15°-45° and internal obstruction heights of 40mm, 50mm, 60mm, and 70mm. The findings were that steeper roof slopes increased the ventilation velocity and decreased with higher obstacle heights, as the recirculation zone behind the building moved upward and expanded with increasing roof pitch. Moey et al. [21] concluded that the saltbox roof configuration offered more velocity and pressure differentials due to the upwind roof height, and overall, they concluded that saltbox roof configurations outperformed gable roof configurations due to their design, which increased pressure differentials and average velocity ratios. In a further study, Moey et al. [22] used the SST k- ω turbulence model with CFD for seven opening

configurations, four unaligned and three aligned openings with varying locations on upwind and leeward walls in an isolated building to find the opening configuration that maximizes ventilation. In the study, it was observed that different span configurations significantly affected the turbulence regions in the building model and that the span locations close to the roof increased the ventilation rate by 6.52% compared to the span locations close to the ground. Furthermore, Ramponi and Blocken [30] performed a set of coupled three-dimensional sRANS simulations for a typical isolated building to improve the accuracy, dependability, and estimation of coupled CFD simulations for cross-ventilation. The accuracy of the CFD calculations was confirmed by rigorous validation using PIV in wind tunnel tests. They conducted this investigation to assess the influence of various computational variables, including the dimensions of the computational domain and turbulence model. A particular focus was dedicated to addressing the issue of oscillatory convergence that was discovered in the simulations.

To the best of the authors' knowledge, there are very few studies in the literature on the effects of window opening geometry on natural cross ventilation, and the existing studies are generally focused on rectangular-based opening geometries. The aim of this study is to present a numerical investigation of natural wind-driven cross ventilation in an isolated building with a variety of window opening shapes, in contrast to the literature, which focuses only on rectangular geometries. This paper consists of four sections. Section 2 presents the material and methods, providing detailed information on the building geometry and configurations, computational flow domains, and grids. The comprehensive findings are provided in Section 3. Lastly, the key results are examined and ultimately concluded by comparing them with one another in Section 4.

2. MATERIALS AND METHODS (MATERİYAL VE METOD)

2.1. Building Geometry and Configurations (Bina Geometrisi ve Konfigurasyonlar)

The geometry of the isolated building utilized in this investigation was based on the reference model presented in the research conducted by Karava et al. [10] and Ramponi and Blocken [30]. The reference building model has dimensions of $L \times W \times H = 100 \times 100 \times 80 \text{ mm}^3$, corresponding to a 1:200 scale reduction and a full-scale size of $20 \times 20 \times 16 \text{ m}^3$. The building model features two

identical openings positioned centrally on opposite walls, each measuring 46 mmx18 mm (WxH). The entire building model contains a uniform wall thickness of 2 mm on the four side walls, ground, and ceiling. To find out how different building opening shapes affect natural cross ventilation, a set of buildings with trapezoidal, triangular, and

hexagonal openings were built using the window opening dimensions (H=18mm, W=46 mm) of the generic isolated building model, which can be seen in Figure 2.

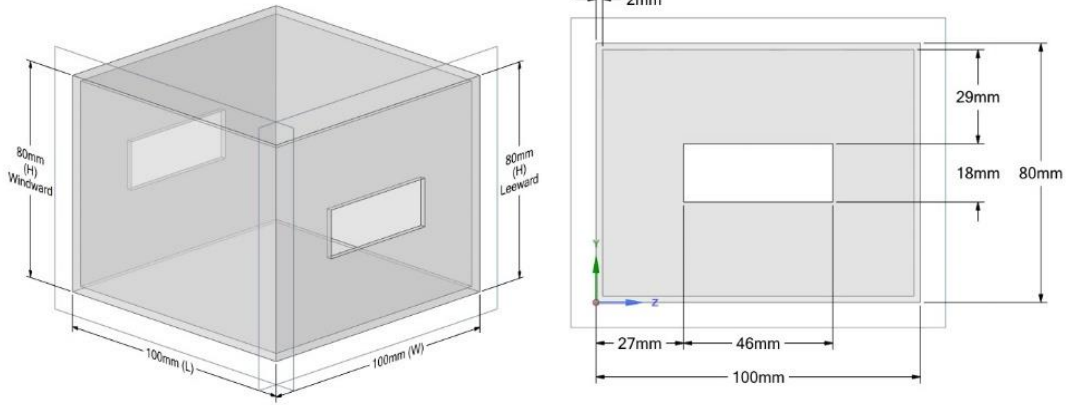


Figure 1. Dimensions of isolated building model (İzole bina modelinin boyutları)

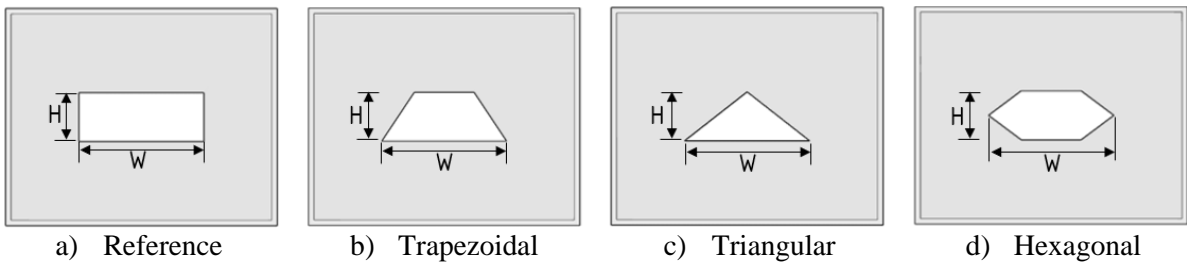


Figure 2. Isolated building models with different window opening geometries (Farklı pencere açıklık geometrilerine sahip izole bina modelleri)

2.2. Computational Flow Domain, Grids and Boundary Conditions (Hesaplamalı Akış Alanı, Gridler ve Sınır Koşulları)

Figure 3 illustrates the isometric view of the rectangular computational domain that was constructed based on the recommendations in the literature [17, 30, 35-37]. The distance from the building to the inlet plane was established at $3H$ (240 mm), where $H=80$ mm, three times the model height, in order to avoid the formation of undesirable gradients in the streamwise direction. Moreover, the length of the building to the outlet plane was established at $15H$ (1200 mm), while $5H$ (400 mm) was placed at the top and side of the domain.

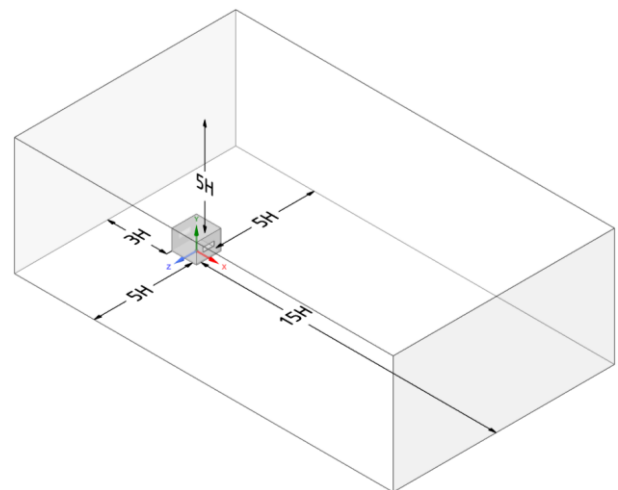


Figure 3. Schematic diagram of the computational domain (Hesaplama alanının şematik diyagramı)

The detailed cross-sectional image of the mesh structure from the vertical mid-plane in the XY directions, as well as close-up views, is presented in Figure 4. In order to get more accurate results in a shorter amount of time, a rectangular body of influence was established to include the building's shape, as seen in this figure. In addition, the flow

surrounding the building was addressed by creating a boundary layer mesh consisting of 10 layers on both the building and the ground, with a first layer thickness of 0.0001 m. The computational grid had around 2.9 million elements.

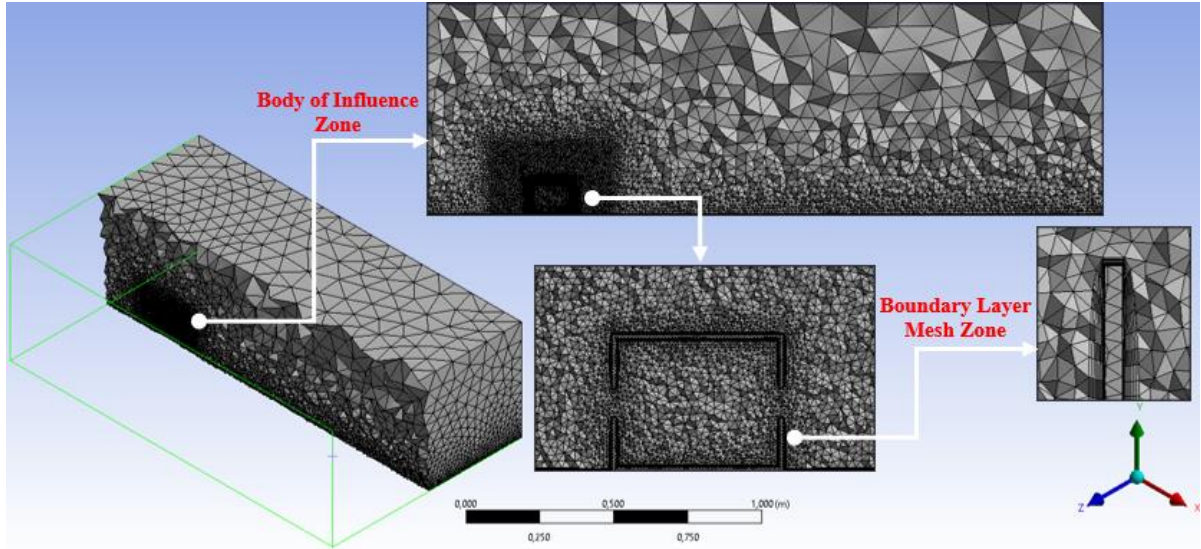


Figure 4. Cross-section and close-up views of the mesh structure (Ağ yapısının kesit ve yakın plan görünüşleri)

The boundary conditions at the inlet plane were established using a set of equations defining the atmospheric boundary layer (ABL) conditions. Afterwards, Equations (1) to (5) were implemented for determining the required input boundary conditions. The equations listed below were utilized as user-defined functions in ANSYS Fluent before the simulation for determining of the velocity profile, specific dissipation rate (ω), and turbulent kinetic energy (k). The equation for the ABL friction velocity (u_{ABL}^*), as shown in Equation (1), incorporated a reference velocity (u_{ref}) of 6.97 m/s, a reference height (z_{ref}) of 0.08 m, the Von Karman constant (κ), and an aerodynamic roughness height (z_0). Subsequently, the velocity profile at the inlet (u) was determined using Equation (2), while the values of u_{ABL}^* , k , and ω were obtained by utilizing

Equation (3) and Equation (4), respectively. In the flow domain, the lateral and upper walls were defined as having zero specific shear stress. Besides, the outlet was described as being a pressure outlet, and the entry plane was designated as a velocity inlet. The inlet conditions were determined from the data in the ABL file, including the velocity magnitude, turbulent dissipation rate, and turbulent kinetic energy. The ground was defined as a boundary wall and subjected to a no-slip requirement. The roughness constant (C_s) was assigned a value of 0.5, resulting in a roughness height of ground sand grain (k_s) of 0.0006 m when plugged into Equation (5) [4, 5, 23, 24].

Table 1. Equations used for the ABL condition (ABL koşulu için kullanılan denklemler)

$u_{ABL}^* = \frac{u_{ref} \cdot \kappa}{\ln \left[\frac{z_{ref}}{z_0} + 1 \right]} \quad (1)$	$k = \frac{(u_{ABL}^*)^2}{\sqrt{C_\mu}} \quad (3)$	$k_s = \frac{9.793 z_0}{C_s} \quad (5)$
$u = \frac{u_{ABL}^*}{\kappa} = \ln \left[\frac{z_{ref}}{z_0} + 1 \right] \quad (2)$	$\omega(z) = \frac{\varepsilon(z)}{C_\mu k(z)} \quad (4)$	$\begin{aligned} \kappa &= 0.42 \\ C_\mu &= 0.09 \\ z_0 &= 0.025 \text{ mm} \end{aligned}$

2.3. CFD Solver Settings (CFD Çözücü Ayarları)

The 3D steady Reynolds averaged Navier-Stokes (RANS) were utilized as the governing equations for the conservation of mass and momentum and had been solved by means of the ANSYS software with $k-\omega$ SST turbulence model. The selection of the appropriate turbulence model is critical to the accuracy of the results obtained from numerical simulations in areas such as aerodynamics, hydrodynamics, and wind engineering, where flow physics and properties are studied [38-45]. The equations that were discretized for pressure-velocity coupling were solved using the SIMPLE method. In addition to this, the Green-Gaussian node-based technique was chosen for spatial discretization to calculate the gradient, while the second-order upwind method was used for all other parameters. In addition to this, convergence was assumed to be obtained when all the scaled residuals leveled off and reached a minimum of 10^{-7} for x , y , and z momentum and 10^{-4} for continuity, k , and ω .

2.4. Validation of the Model (Modelin Doğrulanması)

In Figure 5, the averaged velocity vector fields in the vertical midplane, derived from the CFD simulations conducted in this study and from PIV measurements [9] documented in the literature, were presented. It was demonstrated that the CFD simulation results accurately estimated the most essential flow characteristics, including the nature of the flow distribution pattern within the building and standing vortex flow located at the windward side of the building. Furthermore, the simulations illustrated the presence of a significant downflow in the vicinity of the inlet opening, extending towards the leeward wall. Subsequently, a strong upward movement occurred along the wall, resulting in an inclined flow upward through the outlet opening. The results indicated that the CFD model demonstrated a satisfactory degree of alignment with the experimental data. Accordingly, the aforementioned calculation settings, boundary conditions, and utilized parameters were applied to assess the cross-ventilation flow caused by wind in buildings with varying opening shapes on both the windward and leeward sides.

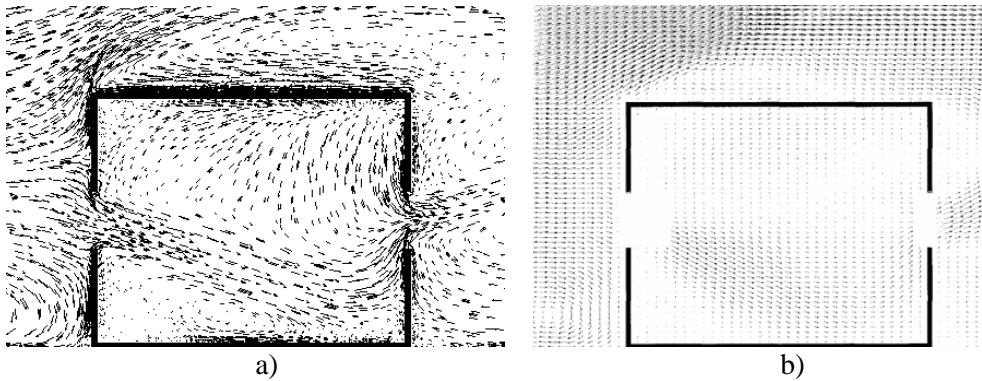


Figure 5. Comparison of the velocity vector distributions in the vertical middle-plane resulting from a) CFD simulation and b) PIV experiment [9] (a) CFD simülasyonu ve b) PIV deneyinden elde edilen dikey orta düzlemdaki hız vektörü dağılımlarının karşılaştırılması [9])

3.RESULTS (BULGULAR)

3.1. Dimensionless Velocity Profile (Boyutsuz Hız Profili)

Figure 6 illustrates the ratio of dimensionless streamwise wind speed (u/u_{ref}) along the horizontal center line of the window opening for various opening geometries. The aforementioned graph was plotted utilizing data obtained from a horizontal line situated between two openings, one situated to the windward side and the other to the leeward side. A dimensionless variable was created by dividing the magnitude of the velocity obtained

within the building by u_{ref} at the height of the building. In order to evaluate the effect of aperture geometries on the indoor airflow inside the building, when the variation of the dimensionless flow velocity in a horizontal line was analyzed, in the range $0 < x/D < 0.5$, a decrease was observed in all curves. In particular, the curve for the triangular geometry showed the sharpest decrease, which decreased to approximately 0.1. The curves of the trapezoid and reference geometries exhibited a similar decrease, while the hexagon curve remained at relatively higher values. At $x/D=0.5$, u/u_{ref} values decreased to their lowest levels. In the range of $0.5 < x/D < 1$, all curves entered an increasing trend

again. Especially when the point $x/D=1$ was approached, all curves reached the range of 0.6-0.7 again. Furthermore, the trend of the airflow velocity demonstrated a U-shaped curve in all cases.

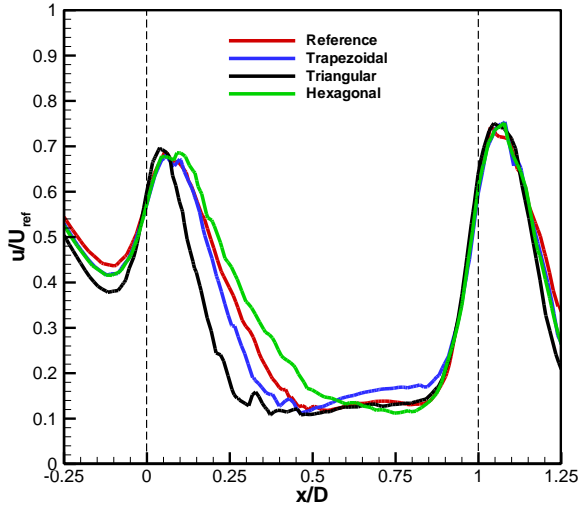


Figure 6. Non-dimensional streamwise wind velocity ratio along the horizontal center line for various window opening shapes (Çeşitli pencere açıklık şekilleri için yatay merkez hattı boyunca boyutsuz akım yönlü rüzgar hızı oranı)

3.2. Velocity and Pressure Contours (Hız ve Basınç Konturları)

The vertical center measurement plane of the building from which the contour results were obtained was given as an example in Figure 7. Additionally, Figure 8 shows the velocity distribution results of the air flow for the building with four different opening geometries. Upon entering the aperture on the windward side, the wind exhibited a high velocity and was observed to generate an immediately apparent downward jet. The direction of the incoming jet was similar for all geometries. However, the size of the jet spread varied depending on geometry. The jet spreading height (H_{jet}) determined for the reference case ($H_{jet-ref} = 0.014$ m) was used as a baseline for comparison with other cases. When trapezoidal geometry was used, the H_{jet} was 98% of the reference height, resulting in a small decrease in H_{jet} with this geometry. This demonstrated that the trapezoidal geometry affected the flow in a very similar way to the reference case. When the triangular geometry was used, the H_{jet} decreased to 61% of the reference height. This result showed that the triangular geometry caused a significant reduction in the H_{jet} and distorted the flow, reducing the propagation of the jet. When hexagonal geometry was used, the H_{jet} increased to 130% of the reference height. This exhibited that the hexagonal geometry caused a significant increase in

the jet height. The H_{jet} was largest for hexagonal geometry with values of $1.30H_{ref}$, while the narrowest was observed in triangular geometry. Figure 8c illustrates the higher velocity in the incoming jet obtained for triangular geometry, also visible in Figure 6, which was directly related to the lesser spreading rate. In triangular geometry, the outgoing jet left the building at a steeper angle. In general, when the airflow reached the outlet, it accelerated to a higher velocity. It was possible to notice a common pattern of airflow, which was that when air with a high-velocity air flowed into the building from the inlet entrance, the velocity reduced as it traveled toward the center of the building, and then it obtained its velocity upon reaching the outside opening.

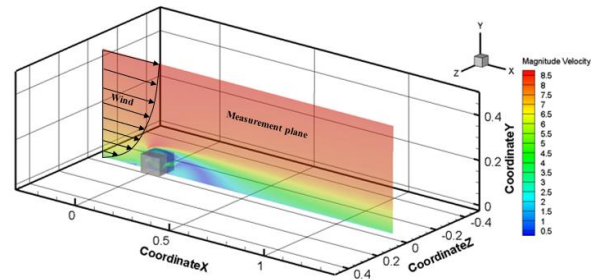


Figure 7. Contour measurement plane at the building center (Bina merkezindeki kontur ölçüm düzlemi)

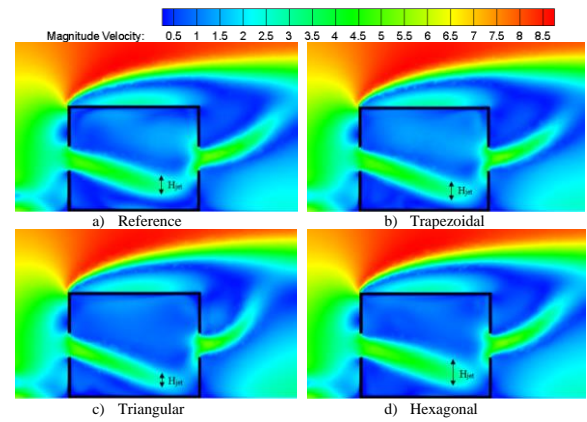


Figure 8. The contours of the mean velocity magnitude in the vertical center plane (Dikey orta düzlemdeki ortalama hız büyüklüğünün konturları)

Figure 9 illustrates the pressure fields for all four configurations. The contours exhibited a satisfactory alignment with the fundamental principle of Bernoulli's equation, which established that the velocity of fluid was reversibly proportional to fluid pressure. Additionally, for all situations, the maximum pressure occurred on the windward wall of the building, resulting from the effect of air impinging upon the windward, as evidenced by the contours of pressure distribution. Additionally, all the results showed large negative pressure magnitudes across the building roof, which was

correlated with the occurrence of a roof separation and reattachment in this zone. Although the pressure distribution within the building was generally consistent, there was a notable increase in this value, particularly in the lower corner of the leeward wall inside the building. This increase was least observed in the result obtained for the triangular geometry.

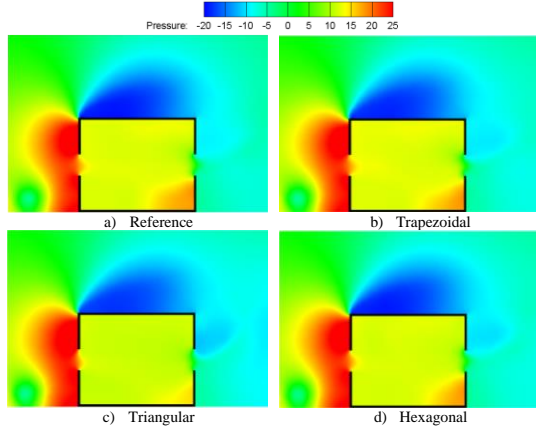


Figure 9. The contours of pressure distributions in the vertical center plane for different window geometries (Farklı pencere geometrileri için dikey orta düzlemdeki basınç dağılımlarının konturları)

3.3. Ventilation Rate (Havalandırma Oranı)

The ventilation rate for a naturally cross ventilated low rise isolated building with one effective inlet and one effective outlet can be determined using the following equations [45].

The airflow coefficient, C_Q was computed by Equation (6) with a reference velocity, u_{ref} of 6.97 m/s and the discharge coefficient, C_d of 0.62 [46].

$$C_Q = u_{ref} C_d \sqrt{\Delta C_p} \quad (6)$$

where, ΔC_p denotes the difference in pressure coefficients between the windward and leeward openings, as defined by Equation (7).

$$\Delta C_p = C_{p,windward} - C_{p,leeward} \quad (7)$$

Moreover, the flow coefficient, C_Q was employed in Equation (8) for the purpose of calculating the actual flow coefficient, C_a .

$$C_a = \frac{C_Q}{1 + C_Q} \quad (8)$$

Lastly, the ventilation rate, Q can be obtained by utilizing Equation (9).

$$Q = u_{ref} A_e C_a \quad (9)$$

where A_e is the area of the opening.

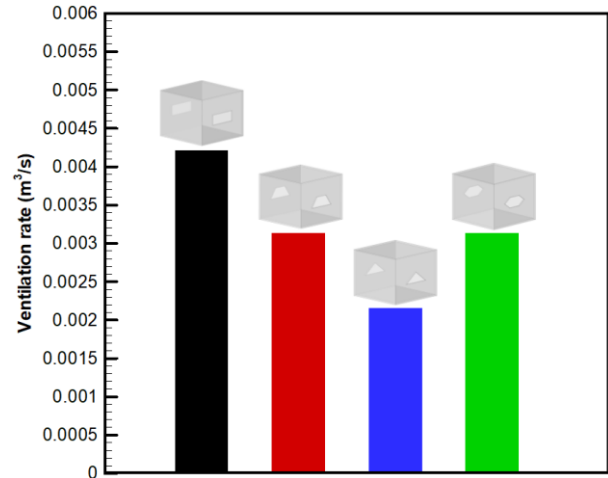


Figure 10. Ventilation rate of isolated building with various window openings (Çeşitli pencere açıklıklarına sahip izole binanın havalandırma oranı)

Figure 10 illustrates the comparison of the ventilation rates obtained for the cross-ventilated isolated building with different window opening geometries in accordance with the equations given above. Comparing the ventilation rates for buildings with reference, trapezoidal, triangular, and hexagonal window geometries revealed that the building with the reference window geometry had the highest ventilation rate. This demonstrated that the reference geometry (rectangular) was the most efficient in terms of ventilation, with a rate of 0.004212 m³/s. The building with a trapezoidal window opening was in second place with a ventilation rate of 0.003136 m³/s, which was slightly lower than that of the reference geometry. On the other hand, the lowest ventilation rate was calculated for the window geometry with a triangular opening, equating to 0.002158 m³/s. This indicated that the triangular opening was the most inefficient in terms of ventilation. In comparison to structures with trapezoidal and triangular windows, the ventilation rate for the hexagonal structure was 0.003134 m³/s, indicating an intermediate performance level. However, this ratio was almost equivalent to the amount of ventilation obtained in the isolated building with trapezoidal windows. Based on these findings, it can be concluded that the window geometry has a significant effect on the natural ventilation performance of the building, and it can also be concluded that the window design should be carefully determined to improve ventilation efficiency. While the reference geometry may be preferred for optimum ventilation, other geometries may be considered for structural or aesthetic needs. However, the triangular geometry

should be avoided in cases where ventilation performance should be prioritized.

4.CONCLUSIONS (SONUÇLAR)

In this study, the situation of wind-driven cross ventilation in an isolated building with four different window opening geometries-rectangular, trapezoidal, triangular, and hexagonal-was investigated numerically. The three-dimensional steady-state CFD simulations were conducted employing the RANS methodology in conjunction with the Shear Stress Transport (SST) $k-\omega$ turbulence model. The key findings were provided as follows:

- The airflow velocity profile showed a U-shaped curve, with a reduction observed in all cases within the range of $0 < x/D < 0.5$.
- Trapezoid and reference geometries demonstrated similar decreases, while the hexagon curve remained relatively higher.
- All curves increased in the range $0.5 < x/D < 1$, reaching values of 0.6-0.7 near $x/D=1$.
- Downward jet with high velocity was noticed upon entering the windward side of the building.
- Jet spreading size varied with geometry, with the reference case having a H_{jet} of 0.014 m.
- Trapezoidal geometry resulted in a small decrease in H_{jet} at 98% of the reference height.
- Triangular geometry reduced H_{jet} to 61% of the reference height, distorting the flow and reducing jet propagation.
- Hexagonal geometry increased H_{jet} to 130% of the reference height, causing a significant increase in jet height.
- Triangular geometry resulted in a higher velocity in the incoming jet, related to a lesser spreading rate.
- A common pattern of airflow was that high-velocity air flowed into the building from the inlet entrance, was reduced towards the center, and gained velocity upon reaching the outside opening.
- Reference geometry achieved the highest ventilation rate ($0.004212 \text{ m}^3/\text{s}$), followed by

trapezoidal, hexagonal, and triangular. The triangular configuration was the least efficient, while the reference configuration was the most efficient.

These findings suggested that window geometry had a significant impact on building ventilation performance. While the reference geometry may be preferred for optimum ventilation, other geometries may be considered for structural or aesthetic needs. However, the triangular geometry should be avoided in cases where ventilation performance should be prioritized. Consequently, careful consideration of window design was essential for optimizing ventilation efficiency.

DECLARATION OF ETHICAL STANDARDS (ETİK STANDARTLARIN BEYANI)

The author of this article declares that the materials and methods they use in their work do not require ethical committee approval and/or legal-specific permission.

Bu makalenin yazarı çalışmalarında kullandıkları materyal ve yöntemlerin etik kurul izni ve/veya yasal-özel bir izin gerektirmediğini beyan ederler.

AUTHORS' CONTRIBUTIONS (YAZARLARIN KATKILARI)

Burak AKTEPE: He performed the literature review and the numerical simulations.

Literatür taramasını ve sayısal simülasyonları gerçekleştirdi.

Hacımurat DEMİR: He analyzed numerical simulation results and performed the writing, editing, and consulting processes.

Sayısal simülasyon sonuçlarını analiz etti ve yazma, düzenleme ve danışmanlık süreçlerini gerçekleştirdi.

CONFLICT OF INTEREST (ÇIKAR ÇATIŞMASI)

There is no conflict of interest in this study.

Bu çalışmada herhangi bir çıkar çatışması yoktur.

REFERENCES (KAYNAKLAR)

- [1] Khan N, Su, Y, Riffat SB. A review on wind driven ventilation techniques. Energy and buildings. 2008; 40(8): 1586-1604.
- [2] Murakami S. Wind tunnel test on velocity-pressure field of cross-ventilation with open windows. ASHRAE transactions. 1991; 97: 525-538.

- [3] Linden PF. The fluid mechanics of natural ventilation. *Annual review of fluid mechanics*. 1999; 31(1): 201-238.
- [4] Karava P, Stathopoulos T, Athienitis AK. Wind-induced natural ventilation analysis. *Solar Energy*. 2007; 81(1): 20-30.
- [5] Tablada A, De Troyer F, Blocken B, Carmeliet J, Verschure H. On natural ventilation and thermal comfort in compact urban environments—the Old Havana case. *Building and Environment*. 2009; 44(9): 1943-1958.
- [6] Ji L, Tan H, Kato S, Bu Z, Takahashi T. Wind tunnel investigation on influence of fluctuating wind direction on cross natural ventilation. *Building and environment*. 2011; 46(12): 2490-2499.
- [7] Kato S, Murakami S, Mochida A, Akabayashi SI, Tominaga Y. Velocity-pressure field of cross ventilation with open windows analyzed by wind tunnel and numerical simulation. *Journal of Wind Engineering and Industrial Aerodynamics*. 1992; 44(1-3): 2575-2586.
- [8] Jiang Y, Alexander D, Jenkins H, Arthur R, Chen Q. Natural ventilation in buildings: measurement in a wind tunnel and numerical simulation with large-eddy simulation. *Journal of Wind Engineering and Industrial Aerodynamics*. 2003; 91(3): 331-353.
- [9] Karava, P. Airflow prediction in buildings for natural ventilation design: wind tunnel measurements and simulation, PhD Thesis, Concordia University, 2008.
- [10] Karava P, Stathopoulos T, Athienitis AK. Airflow assessment in cross-ventilated buildings with operable façade elements. *Building and environment*. 2011; 46(1): 266-279.
- [11] Tominaga Y, Blocken B. Wind tunnel experiments on cross-ventilation flow of a generic building with contaminant dispersion in unsheltered and sheltered conditions. *Building and Environment*. 2015; 92: 452-461.
- [12] Golubić D, Meile W, Brenn G, Kozmar H. Wind-tunnel analysis of natural ventilation in a generic building in sheltered and unsheltered conditions: Impact of Reynolds number and wind direction. *Journal of wind engineering and industrial aerodynamics*. 2020; 207: 104388.
- [13] Evola G, Popov V. Computational analysis of wind driven natural ventilation in buildings. *Energy and buildings*. 2006; 38(5): 491-501.
- [14] Van Hooff T, Blocken B. On the effect of wind direction and urban surroundings on natural ventilation of a large semi-enclosed stadium. *Computers & Fluids*. 2010; 39(7): 1146-1155.
- [15] Meroney RN. (2009, June). CFD prediction of airflow in buildings for natural ventilation. In *Proceedings of the eleventh Americas conference on wind engineering*, Puerto Rico.
- [16] Moey LK, Sing YH, Tai VC, Go TF, Sia YY. Effect of opening size on wind-driven cross ventilation. *International Journal of Integrated Engineering*. 2021; 13(6): 99-108.
- [17] Shirzadi M, Mirzaei PA, Naghashzadegan M, Tominaga Y. Modelling enhancement of cross-ventilation in sheltered buildings using stochastic optimization. *International Journal of Heat and Mass Transfer*. 2018; 118: 758-772.
- [18] Shirzadi M, Mirzaei PA, Tominaga Y. LES analysis of turbulent fluctuation in cross-ventilation flow in highly-dense urban areas. *Journal of Wind Engineering and Industrial Aerodynamics*. 2021; 209: 104494.
- [19] Tong Z, Chen Y, Malkawi A. Defining the Influence Region in neighborhood-scale CFD simulations for natural ventilation design. *Applied Energy*. 2016; 182, 625-633.
- [20] Zobaied A, Tai VC, Go TF, Chong PL, Moey LK. Effect of gable roof with various roof pitches and obstacle heights on natural ventilation performance for an isolated building. *Journal of Mechanical Engineering and Sciences*. 2022; 16(3): 9033-9042.
- [21] Moey LK, Kong MF, Tai VC, Go TF, Adam NM. Effects of roof configuration on natural ventilation for an isolated building. *Journal of Mechanical Engineering and Sciences*. 2021; 15(3): 8379-8389.
- [22] Moey LK, Chan KL, Tai VC, Go TF, Chong PL. Investigation on the effect of opening position across an isolated building for wind-driven cross ventilation. *Journal of Mechanical Engineering and Sciences*. 2021; 15(2): 8141-8152.
- [23] Tai VC, Kai-Seun JW, Mathew PR, Moey LK, Cheng X, Baglee D. Investigation of varying louver angles and positions on cross ventilation in a generic isolated building using CFD simulation. *Journal of Wind Engineering and Industrial Aerodynamics*. 2022; 229: 105172.
- [24] Al-Aghbari OH, Moey LK, Tai VC, Go TF, Yazdi MH. Study on the Impact of Sawtooth Roof Inclination Angles and Asymmetrical Opening Positions for An Isolated Building in Cross Ventilation. *Jordan Journal of Mechanical & Industrial Engineering*. 2022; 16(5).
- [25] Blocken B, Stathopoulos T, Carmeliet J. CFD simulation of the atmospheric boundary layer:

- wall function problems. *Atmospheric environment*. 2007; 41(2): 238-252.
- [26] Blocken B. 50 years of computational wind engineering: past, present and future. *Journal of Wind Engineering and Industrial Aerodynamics*. 2014; 129: 69-102.
- [27] Cook MJ, Ji Y, Hunt GR. CFD modelling of natural ventilation: combined wind and buoyancy forces. *International Journal of Ventilation*. 2003; 1(3): 169-179.
- [28] Van Hooff T, Blocken B. Coupled urban wind flow and indoor natural ventilation modelling on a high-resolution grid: A case study for the Amsterdam ArenA stadium. *Environmental Modelling & Software*. 2010; 25(1): 51-65.
- [29] van Hooff T, Blocken B, Tominaga Y. On the accuracy of CFD simulations of cross-ventilation flows for a generic isolated building: Comparison of RANS, LES and experiments. *Building and Environment*. 2017; 114: 148-165.
- [30] Ramponi R, Blocken B. CFD simulation of cross-ventilation for a generic isolated building: Impact of computational parameters. *Building and environment*. 2012; 53: 34-48.
- [31] Perén JI, Van Hooff T, Leite BCC, Blocken B. CFD analysis of cross-ventilation of a generic isolated building with asymmetric opening positions: Impact of roof angle and opening location. *Building and Environment*. 2015; 85: 263-276.
- [32] Demir H, Aktepe B. (2023). Influence of surrounding buildings on the cross-ventilation of a generic building. *International Congress on Scientific Research-IX*, 166-174
- [33] Blocken B, Stathopoulos T, Carmeliet J. CFD simulation of the atmospheric boundary layer: wall function problems. *Atmospheric environment*. 2007; 41(2): 238- 252.
- [34] Blocken B, Carmeliet J, Stathopoulos T. CFD evaluation of wind speed conditions in passages between parallel buildings—effect of wall-function roughness modifications for the atmospheric boundary layer flow. *Journal of Wind Engineering and Industrial Aerodynamics*. 2007; 95(9-11): 941-962.
- [35] Tominaga Y, Mochida A, Yoshie R, Kataoka H, Nozu T, Yoshikawa M, Shirasawa T. AIJ guidelines for practical applications of CFD to pedestrian wind environment around buildings. *Journal of wind engineering and industrial aerodynamics*. 2008; 96(10-11): 1749-1761.
- [36] Demir H, Aktepe B. (2021). Numerical investigation of the effects of wind flows in different directions on building in the atmospheric boundary layer. *International World Energy Conference (IWEC-2021)*, 6-19.
- [37] Demir H. Numerical investigation of wind loads on building with various turbulence models. *Erciyes Üniversitesi Fen Bilimleri Enstitüsü Fen Bilimleri Dergisi*. 2021; 37(2): 356-366.
- [38] Demir H. (2018). Investigation of Unsteady Aerodynamics of Flexible Wings at Low Reynolds Numbers. PhD. Thesis, Graduate School of Natural and Applied Sciences, Erciyes University, Kayseri, Turkey.
- [39] Demir H, Kaya B. (2023, May). A study on aerodynamic performance of airfoil in ground effect. In *8th International Asian Congress on Contemporary Sciences* (pp. 5-7).
- [40] Özkan R, Genç MS. Aerodynamic design and optimization of a small-scale wind turbine blade using a novel artificial bee colony algorithm based on blade element momentum (ABC-BEM) theory. *Energy Conversion and Management*. 2023; 283: 116937.
- [41] Genç M, Kaynak Ü. (2009). Control of flow separation and transition point over an aerofoil at low Re number using simultaneous blowing and suction. In *19th AIAA Computational Fluid Dynamics* (p. 3672).
- [42] Genç M, Ozisik G, Kahraman N. Investigation of aerodynamics performance of NACA00-12 aerofoil with plain. *ISI Bilimi ve Teknigi Dergisi-Journal of Thermal Science and Technology*. 2008; 28(1).
- [43] Demir H, Özden M, Genç MS, Çağdaş M. (2016). Numerical investigation of flow on NACA4412 aerofoil with different aspect ratios. In *EPJ Web of Conferences* (Vol. 114, p. 02016). EDP Sciences.
- [44] Genç MS. (2009). Control of low Reynolds number flow over aerofoils and investigation of aerodynamic performance. PhD Thesis, Graduate School of Natural and Applied Sciences, Erciyes University, Kayseri, Turkey.
- [45] Demir H, Kaya B. Investigation of the aerodynamic effects of bio-inspired modifications on airfoil at low Reynolds number. *Journal of Mechanical Engineering and Sciences*. 2023; 9715-9724.
- [46] Swami M, Chandra S. (1987). Procedures for calculating natural ventilation airflow rates in buildings. *ASHRAE Final Report, FSEC-CR-163-86*
- [47] Chu CR, Chiu YH, Chen YJ, Wang YW, Chou CP. Turbulence effects on the discharge coefficient and mean flow rate of wind-driven cross-ventilation. *Building and Environment*. 2009; 44(10): 2064-2072.